Available online at www.sciencedirect.com
ScienceDirect
Biochimica et Biophysica Acta 1767 (2007) 143 – 150
Biochimica et Biophysica Acta
BBA
www.elsevier.com/locate/bbabio

The role of Sdh4p Tyr-89 in ubiquinone reduction by the *Saccharomyces cerevisiae* succinate dehydrogenase

Yuri Silkin, Kayode S. Oyedotun, Bernard D. Lemire *

Department of Biochemistry, University of Alberta, Edmonton, Alberta, Canada T6G 2H7

Received 4 August 2006; received in revised form 2 November 2006; accepted 9 November 2006
Available online 6 December 2006

Abstract

Succinate dehydrogenase (complex II or succinate:ubiquinone oxidoreductase) is a tetrameric, membrane-bound enzyme that catalyzes the oxidation of succinate and the reduction of ubiquinone in the mitochondrial respiratory chain. Two electrons from succinate are transferred one at a time through a flavin cofactor and a chain of iron–sulfur clusters to reduce ubiquinone to an ubisemiquinone intermediate and to ubiquinol. Residues that form the proximal quinone-binding site (Q_P) must recognize ubiquinone, stabilize the ubisemiquinone intermediate, and protonate the ubiquinone to ubiquinol, while minimizing the production of reactive oxygen species. We have investigated the role of the yeast Sdh4p Tyr-89, which forms a hydrogen bond with ubiquinone in the Q_P site. This tyrosine residue is conserved in all succinate:ubiquinone oxidoreductases studied to date. In the human SDH, mutation of this tyrosine to cysteine results in paraganglioma, tumors of the parasympathetic ganglia in the head and neck. We demonstrate that Tyr-89 is essential for ubiquinone reductase activity and that mutation of Tyr-89 to other residues does not increase the production of reactive oxygen species. Our results support a role for Tyr-89 in the protonation of ubiquinone and argue that the generation of reactive oxygen species is not causative of tumor formation.

Keywords: Mitochondria; Yeast; Succinate:ubiquinone oxidoreductase; Complex II

1. Introduction

Succinate dehydrogenase (SDH)[1] of the mitochondrial respiratory chain (MRC) is intriguing because of its importance in energy generation and in mitochondria-related diseases. SDH, also referred to as complex II, functions as a succinate–ubiquinone oxidoreductase, oxidizing succinate to fumarate and reducing ubiquinone to ubiquinol. The yeast enzyme, like its mammalian counterpart, is encoded by four nuclear genes, *SDH1-4*. Electron transport from the succinate-binding site to the first or proximal quinone-binding site (Q_P) is along a chain of redox groups that includes a covalently attached FAD and three iron–sulfur clusters. In addition to these redox groups, the yeast enzyme contains a *b*-type heme and a second or distal quinone-binding site (Q_D), the roles of which remain controversial [1].

SDH is composed of two domains; the catalytic domain, containing the flavoprotein Sdh1p and the iron–sulfur Sdh2p subunits, is linked to the mitochondrial inner membrane surface by association with the membrane domain. The membrane domain is composed of the two hydrophobic subunits, Sdh3p and Sdh4p, which house the heme and the quinone-binding sites. SDH structures of the *Escherichia coli* [2,3], the porcine heart [4], the chicken heart [5] and the *Saccharomyces cerevisiae* [6] enzymes have been determined or modeled. Despite this abundance of structural information, the mechanistic details of catalysis, especially those that occur in the membrane domain, remain poorly understood.

Heterozygous mutations in the human *SDHB*, *SDHC* or *SDHD* genes cause paraganglioma or pheochromocytoma [7–9]. Pheochromocytomas are catecholamine-secreting tumors that arise in the adrenal medulla and are usually benign. They can develop in extra-adrenal ganglia, in which case they are often referred to as paraganglioma. The most common site of paraganglioma is the carotid body, an organ involved in oxygen sensing. Thus, it has been proposed that the SdhB, SdhC, and SdhD subunits may be critical components of an oxygen-sensing system [10]. Interestingly, paraganglioma appears to be

* Corresponding author. Tel.: +1 780 492 4853; fax: +1 780 492 0886.
E-mail address: bernard.lemire@ualberta.ca (B.D. Lemire).

0005-2728/$ - see front matter © 2006 Elsevier B.V. All rights reserved.
doi:10.1016/j.bbabio.2006.11.017

about 10-fold more prevalent in residents of the Andean mountains, high altitude dwellers who chronically experience hypoxia [11].

SDH mutations are also associated with premature aging. The *mev-1*(*kn1*) mutation (Gly71Glu) in the *Caenorhabditis elegans cyt-1* gene, which encodes an Sdh3p homolog, results in animals that are hypersensitive to methyl viologen (paraquat, a free radical generator) and to hyperoxia [12]. Mutant animals exhibit signs of premature aging, defects in apoptosis and have a shortened lifespan that can be extended with free radical scavenging compounds [13,14]. The *mev-1* mutation, which affects an amino acid at the Q_P site, leads to an elevated production of superoxide [15].

Three models have been proposed to explain how SDH dysfunction can lead to tumor development [16]. First, defects in SDH or elsewhere in the MRC may render cells more resistant to apoptosis, contributing to tumor development. In a second model, decreased or defective SDH activity might lead to an increased production of reactive oxygen species and to an aberrant regulation of apoptosis or response to hypoxia [17]. Finally, succinate, which accumulates as a result of SDH dysfunction, might lead to the stabilization and activation of hypoxia inducible factor (HIF) by directly inhibiting HIF prolyl hydroxylase [18,19]. The prolyl hydroxylase is responsible for oxygen-dependent posttranslational modifications of HIF that promote its translocation to the nucleus.

To better understand the molecular bases of pathogenic SDH mutations, we have investigated the role of the Q_P site residue Sdh4p Tyr-89. Paraganglioma develops when the equivalent tyrosine is mutated to cysteine in the human SDHD subunit. We substituted several residues at position 89 and measured SDH assembly, SDH activity, sensitivity to oxidative stress and superoxide production. Our data indicate that Tyr-89 has an essential role in ubiquinone reduction. We did not detect increased superoxide production in any of the Tyr-89 mutant enzymes, arguing against a causative role for reactive oxygen species in tumor formation.

2. Materials and methods

2.1. Strains, media and culture conditions

The *S. cerevisiae* strain, YPH499 (*MATα, ura3-52, lys2-801amber, ade2-101ochre, his3Δ200, leu2Δ1, trp1Δ63,* ρ+) was obtained from Stratagene (La Jolla, CA). sdh4w5 (YPH499, *sdh4::TRP1*) contains a complete deletion and replacement of the *SDH4* gene by the selectable marker *TRP1*. The *E. coli* strain DH5α was used for all genetic manipulations [20]. The yeast media (YPD, YPG, SD, SG, YPGal, SGal, YPD+0.6%D and semisynthetic medium SS) and culture conditions have been reported [20,21]. The respiratory capacities of mutants were determined as the maximal optical densities attained in SS medium with limiting galactose (0.1–0.3%) after ~100 h of growth [20]. Oxygen or paraquat sensitivity were measured by growing aliquots of serially-diluted cultures on plates incubated at 30 °C in an anaerobic jar continuously flushed with ~20 ml/min pure oxygen or in the presence of 0.5–1.0 mM paraquat [22].

2.2. Construction of mutants

Site-directed mutagenesis was performed by PCR as described [23] using two complementary mutagenic primers and forward and reverse flanking primers containing *Bgl*II and *Xho*I restriction sites, upstream and downstream of the *SDH4* gene, respectively. pSDH4–17 is a 6.1-kb plasmid in the vector pRS416 containing the entire *SDH4* gene (546 coding nucleotides) as well as 156 bp upstream and 588 bp downstream. Mutations were confirmed by sequencing the entire insert in both directions. Sequencing reactions were performed by the Department of Biochemistry DNA Core Facility (University of Alberta, Edmonton, AB, Canada).

Saturation mutagenesis was performed with the forward oligonucleotide (5′-CTCTTTCAGAAATNVNATCGGTGATACAAGAG-3′), which contains a degenerate codon (underlined). The degenerate NVN (*N*=any nucleotide, V=A, G or C) codon can introduce all possible amino acid substitutions at position 89 in Sdh4p except tyrosine. A complementary oligonucleotide was also prepared. PCR products were separated electrophoretically in agarose gels, excised and purified with the QIAEX® II gel extraction kit (Qiagen Inc.), digested with *Bgl*II and *Xho*I and ligated into pRS416 cut with *Bam*HI and *Xho*I to create a library of *SDH4* codon 89 mutants. The library was transformed into sdh4w5 and plated on SG plates containing 0.1% glucose. The 20 largest colonies from over 1600 transformants were selected. The plasmids were recovered and sequenced (coding, promoter and downstream sequences).

2.3. Computational methods

All molecular dynamics simulations were carried out using the GROMACS 3.3 package [24] with the GROMOS96 force field. Simulations were performed under the conditions of constant pressure, constant temperature, and constant particle number (*NpT* ensemble). Temperature was set at 325 K using the Berendsen thermostat, while anisotropic pressure was maintained at 1 atm using the Parrinello–Rahman barostat. The yeast SDH (coordinates 1PB4 [6]) was inserted into dipalmitoylphosphatidylcholine (DPPC) bilayer, solvated with simple point charge (SPC) water. Sdh1p was removed to reduce the intensity of the computation as it does not contribute to quinone binding. The starting membrane model was a pre-equilibrated 64 DPPC [25], which was modified to 271 DPPC and 23,553 SPC water in order to accommodate the protein. The protein was position-restrained for 500 ps to allow the lipid to equilibrate. This was followed by a 500 ps equilibration of the whole system without restraints. For free energy calculations, the system was further equilibrated for 500 ps, followed by 1 ns production runs. A conformational search simulation was performed to determine if ubiquinone binding differed in the mutant Q_P sites. The mutant SDHs were equilibrated into a solvated bilayer and an extended simulation of 2 ns was performed. The mutant SDH structures were then superimposed on the wild type and the ubiquinone binding sites compared. All molecular dynamics computations were carried out on the University of Alberta 3.8 GHz Intel Pentium 4 processor 44-node Linux cluster.

The mutational free energy changes in the native and denatured states (Fig. 1) are calculated by the thermodynamic integration (TI) equation:

$$\Delta G = \int_0^1 \left\langle \frac{\partial H(\lambda)}{\partial \lambda} \right\rangle_\lambda d\lambda \tag{26}$$

where $H(\lambda)$ is an intermediate Hamiltonian and λ is a coupling constant between the wild-type ($\lambda=0$) and mutant ($\lambda=1$). The bracket $< >_\lambda$ denotes ensemble average for the system characterized by the Hamiltonian $H(\lambda)$. $H(\lambda)$ is scaled from $\lambda=0$ to $\lambda=1$ by increments $\delta\lambda=0.04$ (slow-growth, 25 intermediate λ states). Short peptide models were used to model the denatured state and reduce the intensity of the computations [26].

2.4. Isolation of mitochondria and enzyme assays

Cultures grown in YP+0.6%D to late stationary phase (72–96 h were harvested by centrifugation, washed with ddH_2O, and resuspended in a HEPES buffer (20 mM HEPES–KOH, pH 7.4, 1 mM EDTA) at 0.6 g/ml yeast cells (wet weight). Complete protease inhibitor cocktail tablets (Roche Diagnostics) and 1 mM phenylmethylsulfonyl fluoride (PMSF) were added just prior to cell lysis by three passes (at 16,000–18,000 psi) through a French pressure cell (American Instrument Company, Silver Spring, Maryland) [27]. Enzyme assays were performed as described [20]. Superoxide production was assayed as the malonate-sensitive, superoxide dismutase-sensitive reduction of cytochrome *c* using superoxide dismutase from bovine erythrocytes (catalog number S-2515,

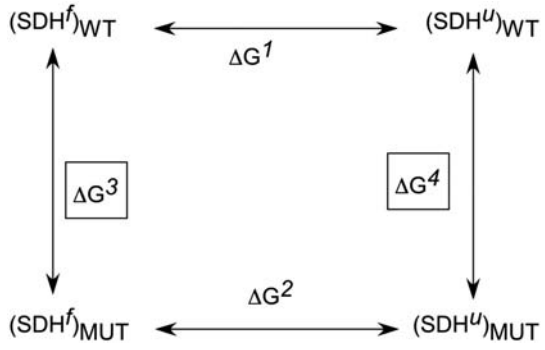

Fig. 1. The thermodynamic cycle used in the free energy calculation. A capped 25-amino acid residue peptide in an extended structure was used to model the denatured state [26,36]. To validate the approach, the denatured state of the wild type protein containing a Y89A mutation was simulated *in vacuo* at 1000 K for 2 ns and then solvated in DPPC. The result of the relative free energy calculated with this approach was compared with 5 to 25-residue peptide models; the 25-residue peptide was found to be in close agreement with the simulated denatured state of the protein [26]. In addition, our results show that the 25-mer unfolded state model is the most stable calculation and demonstrates the lowest hysteresis. For the mutants, capped 25-residue peptides with the mutation in the middle, were used to model the denatured states. The free energy difference between the wild-type and mutant proteins ($\Delta\Delta G$) is defined as the difference between the mutational free energy changes in the native state and in the denatured state [26]: $\Delta\Delta G^f = \Delta G^1 - \Delta G^2 = \Delta G^3 - \Delta G^4$. $(SDH^f)_{WT}$ and $(SDH^u)_{WT}$ are the folded and the unfolded wild type proteins, respectively, while $(SDH^f)_{MUT}$ and $(SDH^u)_{MUT}$ correspond to the folded and the unfolded mutant proteins, respectively. The alchemical paths ΔG^3 and ΔG^4 were calculated by molecular dynamics.

Sigma) in the presence of 1 mM KCN [22]. All activities measured were confirmed to be succinate-dependent.

2.5. Miscellaneous methods

Measurements of covalently attached flavin and protein contents, yeast and *E. coli* transformation, and recombinant DNA methods have been described [28].

3. Results

Sdh4p Tyr-89 was substituted with phenylalanine and cysteine. A phenylalanine removes the hydrogen bonding properties of the tyrosine side chain while preserving the aromatic ring; this should result in a minimal structural perturbation. Tyr-89 was also substituted with cysteine because in humans, SdhD Y114C is linked to head and neck paraganglioma [29].

To discover whether any other residues could effectively substitute for Tyr-89, we constructed degenerate oligonucleotides that could lead to the insertion of all possible amino acids at codon 89. The oligonucleotides were used in PCR mutagenesis to create a pool of codon-89 mutants. We transformed this pool into the *SDH4* null strain sdh4w5 and obtained more than 1600 transformants. These were tested for growth on SG plates containing 0.1% glucose. Respiration deficient transformants form small colonies by fermenting glucose; respiration competent transformants continue growing to form larger colonies. We recovered and sequenced the plasmids from the 20 largest colonies; four of these encoded a tyrosine at position 89 and were not further analyzed (Table 1). The Y89I mutant was unexpected because the isoleucine side chain is apolar. To confirm the partial complementation for respiratory growth, we isolated the plasmid and re-transformed it into fresh sdh4w5. These new transformants could also form larger colonies on SG plates containing 0.1% glucose. The plasmid was re-sequenced and the nucleotide changes confirmed (number 10, Table 1).

We measured the growth yields of the Tyr-89 mutants on semisynthetic medium containing 0.1–0.3% galactose. An initial fermentative growth is followed by a respiratory phase when fermentable carbon source is limiting. Respiratory function contributes to the final growth yield even if the amount of respiratory function is insufficient to support growth in the absence of fermentation, as it is in the Tyr-89 mutants. The optical densities at 600 nm of late stationary phase cultures were measured (Fig. 2). The *SDH4* deficient strain containing an empty vector has a growth yield of 16% compared to when it contains the wild type *SDH4* gene. The growth yields of the Y89C and Y89F mutants do not differ from that of the *SDH4* deletion strain. The Y89I, Y89T, Y89S, and Y89R mutants have growth yields ranging from 24 to 39% of wild type, significantly more than the *SDH4* deletion strain, indicating the mutant enzymes support some respiratory growth. The respiratory capabilities of all mutants correlate well with their colony sizes on SG plates containing 0.1% glucose.

To measure the effects of the mutations on enzyme assembly, we measured the levels of covalent FAD in mitochondrial membranes (Table 2). SDH is the major covalent flavoprotein in *S. cerevisiae* and the covalent flavin levels in mitochondrial membrane fractions reflect the extent of SDH assembly [30]. The covalent FAD contents of the mutant membranes are

Table 1
Plasmids recovered from the saturation mutagenesis

	Codon-89 sequence	Amino acid substitution	Additional mutations[a]
1	AGG	Arg	
2	CTG	Leu	C→T at +266 (T89I). Not further analyzed.
3	ACG	Thr	Single base deletion at +531. Not further analyzed.
4	GGG	Gly	G→A at +231 (L77I). Not further analyzed.
5	CCC	Pro	C→T at −23 and T→C at −50. Not further analyzed.
6	TCG	Ser	
7	TCC	Ser	A→G at +490 (S133G). Not further analyzed.
8	AGG	Arg	Multiple mutations. Not further analyzed.
9	AGA	Arg	
10	ATA	Ile	Silent T→C transition at +258 (A86A).
11	AGA	Arg	
12	ACT	Thr	
13	TCG	Ser	
14	AGG	Arg	
15	ACG	Thr	
16	CGG	Arg	

[a] The nucleotides are numbered from the first position of the start codon.

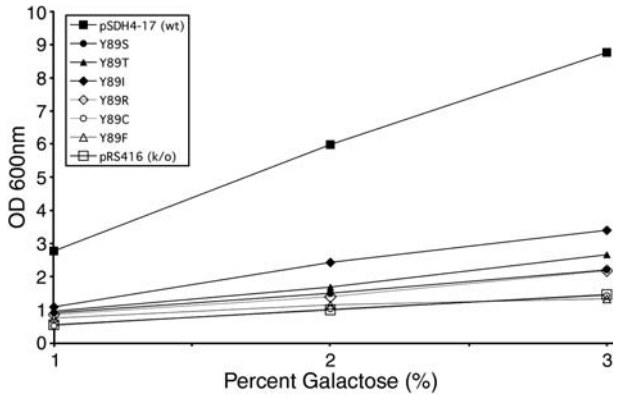

Fig. 2. Growth of strains on galactose medium. Strains were grown at 30 °C on semisynthetic liquid medium containing 0.1–0.3% galactose and the optical densities at 600 nm were measured. The relative growth yields were calculated using the final optical density values on 0.3% galactose. Each point represents the average of 4 or more independent cultures.

slightly diminished compared to the wild type levels, ranging from 60% (Y89T) to 85% (Y89S), indicating that enzyme assembly is largely unaffected by the Tyr-89 mutations.

The malonate-sensitive, succinate-PMS/DCPIP reductase assay measures the activity of the SDH catalytic domain attached to the membrane; the enzyme does not require a catalytically competent membrane domain for this activity. The specific activities of all mutants are lower than the wild type, ranging from 41% (Y89F) to 69% (Y89I) (Table 2), indicating SDH assembly is not greatly impaired (~2-fold or less). There is residual covalent flavin and malonate-sensitive, succinate-PMS/DCPIP reductase activity in the deletion mutant, which we suspect are attributable to the expression of one or both of the Sdh4p paralogs found in the *S. cerevisiae* genome; the amount of residual SDH is strain-dependent [1].

To further explore the effects of the Tyr-89 mutations on SDH stability, we compared the calculated unfolding free energies of the mutants to the wild type using the equation: $\Delta\Delta G = \Delta G_{MUT} - \Delta G_{WT}$. A negative free energy difference ($\Delta\Delta G$) indicates that the mutation destabilizes the protein. The Tyr-89 mutations have minor effects on enzyme stability, with free energy changes of less than 1.5 kcal mol^{-1} (Table 3). A buried intramolecular hydrogen bond is estimated to increase protein stability by ~1.5±1.0 kcal mol^{-1} [31]. The magnitudes of the unfolding free energy changes associated with the Tyr-89 mutations suggest that any changes to the enzyme structure are minor. The flavin contents, the succinate-PMS/DCPIP activities and the energy calculations all suggest that the Tyr-89 mutations do not induce large structural perturbations. None of the mutations reduces the turnover numbers for the mutant enzymes in the succinate-PMS/DCPIP reductase assay by more than 1.7-fold.

Table 3
Stability of the Tyr-89 mutants calculated from molecular dynamics simulations

Mutant	$\Delta\Delta G$ [a] (kcal mol^{-1})
Y89F	−0.27
Y89C	−0.63
Y89S	−1.15
Y89I	−1.40
Y89T	−1.44
Y89R	−1.51

[a] The unfolding free energies are calculated using the equation: $\Delta(\Delta G) = \Delta G_{MUT} - \Delta G_{WT}$.

To explore the effects of the mutations on electron transfer, we assayed the succinate-dependent reduction of either exogenous quinone (succinate-DB reductase activity) or of exogenous cytochrome *c* (succinate-cytochrome *c* reductase activity). The latter assay depends on complexes II and III of the respiratory chain and on endogenous ubiquinone. In sharp contrast to the succinate-PMS/DCPIP reductase activities, which are reduced by 2-fold or less, the quinone reductase activities were drastically reduced (Table 4). The succinate-cytochrome *c* reductase activities of the Tyr-89 mutants are all reduced by 20-fold or greater and are just slightly higher than that observed in the *SDH4*-deficient control.

To determine whether the Tyr-89 mutations reduce the affinity of the Q_P sites for quinone, we measured the succinate-DB reductase activities in the presence of higher concentrations of DB. As expected, the activity of the wild type enzyme is not

Table 2
Assembly of the mutant enzymes

Strain	Covalent FAD [a]	Specific activity [b]	Turnover number [c]
Y89-wild type	16±1 (100%)	80±10 (100%)	4800±600 (100%)
Y89S	13.7±0.3 (85%)*	50±5 (64%)*	3600±300 (75%)*
Y89T	9.7±0.4 (60%)*	36±3 (47%)*	3800±200 (78%)*
Y89I	10.7±0.7 (67%)*	54±7 (69%)*	5000±400 (104%)
Y89R	10.6±0.5 (66%)*	39±4 (51%)*	3700±200 (77%)*
Y89C	14±1 (84%)*	42±4 (54%)*	3100±300 (63%)*
Y89F	11.2±0.8 (70%)*	32±3 (41%)*	2800±200 (58%)*
Δ*SDH4*	4.2±0.3 (26%)*	8.1±0.7 (10%)*	1000±100 (20%)*

[a] Covalent flavin contents are expressed as pmol FAD mg of protein^{-1}. Each value represents the mean of quadruplicate determinations±S.E.

[b] Specific activities are expressed as μmol of PMS-mediated DCPIP reduced min^{-1} mg of protein^{-1}.

[c] Turnover numbers are expressed as μmol of PMS-mediated DCPIP reduced min^{-1} μmol of covalent FAD^{-1}.

* $P<0.01$ using a two-tailed unpaired Student's *t*-test compared to the wild-type.

Table 4
Quinone-reductase activities of the mutant enzymes

Strain	Succinate-DB reductase activity [a]	Succinate-cytochrome *c* reductase activity [b]
Y89-wild type	3600±700 (100%)	2400±300 (100%)
Y89S	470±80 (13%)*	77±7 (3%)*
Y89T	440±90 (12%)*	66±4 (3%)*
Y89I	500±100 (14%)*	120±30 (5%)*
Y89R	470±90 (13%)*	100±10 (4%)*
Y89C	380±40 (11%)*	37±5 (2%)*
Y89F	190±40 (5%)*	26±3 (1%)*
Δ*SDH4*	170±40 (5%)*	38±7 (2%)*

[a] Activities are expressed as μmol of DB-mediated DCPIP reduced min^{-1} μmol of covalent FAD^{-1}.

[b] Activities are expressed as μmol of cytochrome *c* reduced min^{-1} μmol of covalent FAD^{-1}.

* $P<0.01$ using a two-tailed unpaired Student's *t*-test compared to the wild-type.

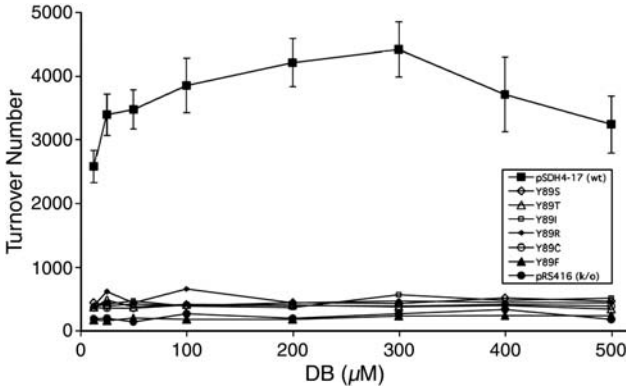

Fig. 3. Dependence of SDH turnover number on decylubiquinone concentration. The succinate-DB reductase assay is normally performed with 50 μM DB (final concentration). Activity values are expressed as turnover numbers (μmol DB reduced min^{-1} μmol of covalent FAD^{-1}). Each point represents the average of 4 or more independent measurements.

increased by increasing the DB concentration from 50 to 500 μM (Fig. 3). In addition, pre-incubation of the mutant enzymes with 250 μM DB also does not increase DB reductase activity (not shown). These data indicate that the reduced quinone reductase activities of the mutants are not due to a decreased affinity of the Q_P sites for quinone substrates. The low residual activities of the Tyr-89 mutants prevented us from determining their apparent affinities for DB.

We explored the structure of quinone-binding site in the wild type and the mutants computationally. The starting coordinates were the S. cerevisiae SDH model 1PB4 [6]. We predicted that the Tyr-89 mutations might cause ubiquinone to bind in a different position within the Q_P site or to adopt a different orientation within while bound at the same location. Our computational results argue against large changes in the architecture of the Q_P site. Additionally, there were no significant differences in the position or orientation of bound

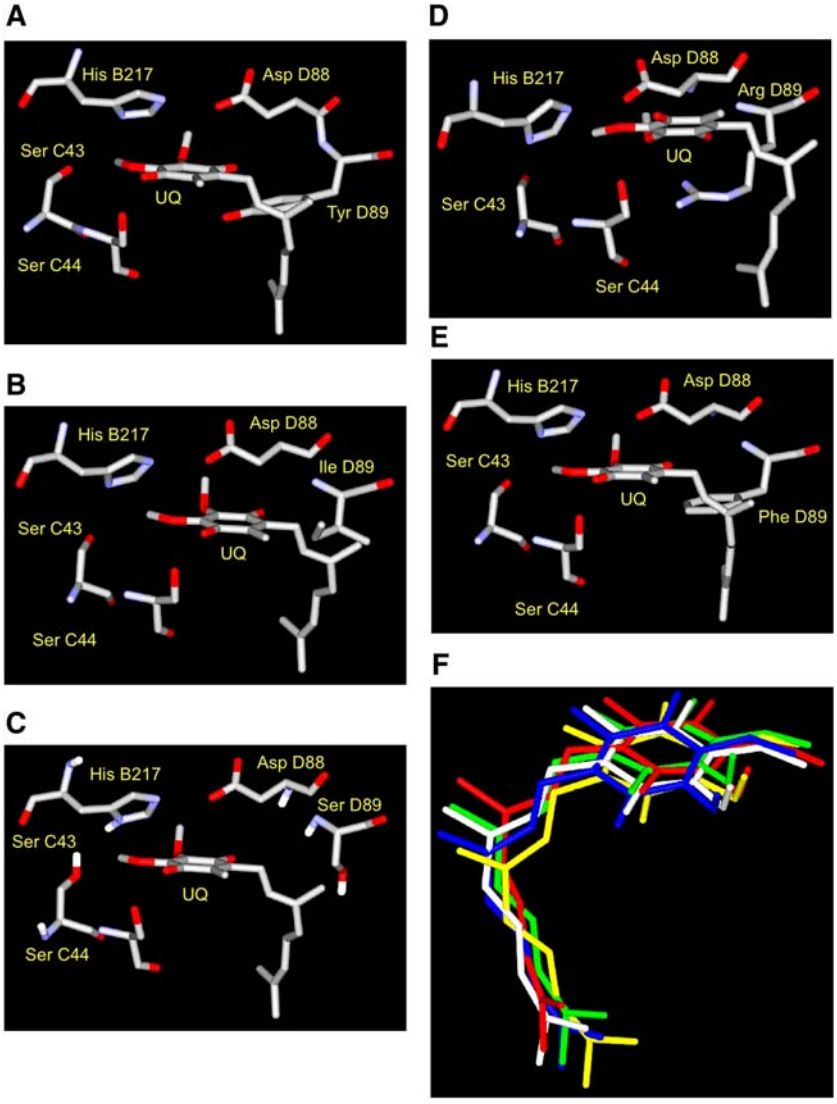

Fig. 4. Effect of Sdh4p Tyr-89 (Tyr D89) mutations on the ubiquinone binding pocket. The structures of the wild type and mutant proteins were simulated for 2 ns in solvated DPPC. Panels A to E depict the environments of bound quinone in the wild type enzyme (A), and the Y89I (B), Y89S (C), Y89R (D), and Y89F (E) mutants at the end of the simulation. Panel F depicts the superposed ubiquinone positions from the averaged, minimized structures of the last 500 ps of simulation. White, wild type; red, Y89F; green, Y89I; blue, Y89R; yellow, Y89S.

Table 5
Superoxide generation by the mutant enzymes

Strain	Total activity [a]	Complexes II+III-dependent activity [b]	Superoxide-mediated activity [c]
Y89-wild type	2257±300 (100%)	2204 (98%)	53 (2%)
Y89S	69±7 (3%)*	62 (90%)	7 (10%)
Y89T	63±4 (3%)*	58 (92%)	5 (8%)
Y89I	112±30 (5%)*	104 (93%)	8 (7%)
Y89R	94±10 (4%)*	83 (89%)	10 (11%)
Y89C	30±5 (2%)*	23 (76%)	7 (24%)
Y89F	24±3 (1%)*	18 (72%)	7 (28%)
Δ*SDH4*	40±7 (2%)*	31 (78%)	9 (22%)

[a] Activities are expressed as the total μmol of cytochrome *c* reduced min^{-1} μmol of covalent FAD^{-1}. Percentages compare activities to the wild type level.
[b] Activities are expressed as μmol of cytochrome *c* reduced min^{-1} μmol of covalent FAD^{-1} by complex III. Percentages refer to the portion of the total activity.
[c] Activities are expressed as the μmol of cytochrome *c* reduced min^{-1} μmol of covalent FAD^{-1} by a superoxide dismutase-sensitive pathway. Percentages refer to the portion of the total activity.
* $P<0.01$ using a two-tailed unpaired Student's *t*-test compared to the wild-type.

quinone in the mutant enzymes; within the time frame of the simulation (2 ns), the equilibrium position coincided with the original position of the Q [2] (Fig. 4). That the quinone remains bound suggests that intermolecular forces other than hydrogen-bonding (electrostatic and van der Waals forces such as ring stacking) contribute significantly to quinone binding. A more detailed analysis of the forces contributing to quinone binding will be presented elsewhere.

Superoxide production was assayed as the malonate-sensitive, superoxide dismutase-sensitive cytochrome *c* reductase activity in the presence of cyanide to inhibit cytochrome *c* oxidase [22]. Two pathways of electron transfer can be used reduce cytochrome *c*: in the first, electrons flow through SDH to ubiquinone, through complex III and to cytochrome *c*; in the second pathway, a superoxide anion directly reduces cytochrome *c*. Superoxide dismutase will inhibit the second pathway by converting superoxide into hydrogen peroxide, but will have no effect on the first pathway. In each of the Tyr-89 mutants, we measured significantly decreased rates of superoxide production compared to the wild type (Table 5). It should be noted, however, that the superoxide-mediated pathway accounted for a larger fraction of the total enzyme activity in the mutants than in the wild type.

4. Discussion

Our results indicate that Sdh4p Tyr-89 is essential for efficient quinone reductase activity. In our saturation mutagenesis of codon 89, only a tyrosine was found to support full respiratory growth; all other substitutions completely abolished growth on SG medium. However, when a small amount of glucose was added to the SG medium, we observed a variety of colony sizes, indicating that some of the colonies had limited respiratory capacity. When these Tyr-89 substitutions were recovered and the plasmids sequenced, we found that Ile, Ser, Thr, or Arg substitutions were able to support limited SDH activity that was 2–3 fold higher than in the knockout strain (Table 4). These observations suggest that the tyrosine side chain has some chemical or structural property that is uniquely suited to its role in catalysis. This is consistent with the observation that in all succinate:ubiquinone oxidoreductase sequences examined to date, a tyrosine is absolutely conserved.

The dramatic losses of quinone reductase activity observed in the Tyr-89 mutants are not due to disruption of SDH assembly or stability. For example, when Tyr-89 is replaced with Phe or Cys, the enzymes are almost completely inactive as quinone reductases (Table 4), yet assembled with reasonable efficiency as measured by covalent flavin contents and by membrane associated succinate-PMS/DCPIP reductase activities (Table 2). Our computational studies also support this conclusion; the 6 amino acid substitutions we examined do not result in large changes in unfolding free energies (Table 3). Therefore, we conclude that the loss of Tyr-89 has only minor structural consequences but severe catalytic ones.

The precise mechanisms of SDH-mediated ubiquinone reduction remain poorly understood. When the *E. coli* SDH was crystallized and its structure solved, density corresponding to one molecule of ubiquinone was found at the Q_P site [2]. It is at this site that the inhibitors TTFA (thenoyl trifluoroacetone) and carboxin bind to the avian and pig enzymes [4,5]. The *E. coli* structure revealed that SdhD Tyr-83 and SdhB Trp-164 are direct ligands of the O1 atom of ubiquinone [2]. It was noted that Tyr-83 also formed a hydrogen bond with SdhC Arg-31, which could reduce the pK_a of the tyrosine side chain, allowing it to serve as direct proton donor during quinone reduction [2]. In the *E. coli* structure, no amino acid side chain was located in the vicinity of the ubiquinone O4 carbonyl oxygen, leading to the suggestion that a water molecule might serve as proton donor. In our model of the *S. cerevisiae* SDH, Sdh4p Tyr-89 and Sdh3p Ser-44 are within hydrogen bonding distance of the O1 and O4 atoms of the docked ubiquinone, respectively [6].

More recently, a mechanism for the reduction of ubiquinone by the *E. coli* SDH has been proposed based on additional structural and computational studies [3]. In this mechanism, the ubiquinone is believed to rotate from an initial binding site called Q_1, which corresponds to the position of the ubiquinone seen in the original crystal structure [2], to a computationally-determined second site called Q_2 in which the O4 carbonyl group now hydrogen bonds with SdhC Ser-27 and the O3 methoxy group hydrogen bonds with SdhB His-207. The Q_2 site more closely resembles the position of the docked ubiquinone in our yeast model [6]. The hydrogen bond between SdhD Tyr-83 and the O1 carbonyl group of ubiquinone serves to anchor the quinone during the rotation. Following movement into the Q_2 position, the ubiquinone is reduced by the almost simultaneous delivery of an electron from each of the [3Fe–4S] cluster and the heme. Protonation via water-39 disrupts the hydrogen bonds with Tyr-83, Ser-27 and His-207 and allows ubiquinol to depart.

Our data are consistent with a more significant role for Sdh4p Tyr-89 than what is proposed for *E. coli* SdhC Tyr-83 [3]. Tyr-89 has an essential role in quinone reduction in the yeast SDH. The catalytic activities of the mutant enzymes are

not stimulated by 5-fold higher DB levels, suggesting that the drops in activity in the Tyr-89 mutants cannot simply be ascribed to a decreased affinity for quinone. In other quinone-binding site mutations we have investigated, activities could be increased with higher substrate concentrations [32]. Furthermore, our computational studies do not indicate that the Tyr-89 mutations significantly interfere with ubiquinone binding; the quinone remains at the initial binding site in the 1PB4 coordinates; this site corresponds to the Q_2 position of the *E. coli* SDH [2]. The simplest explanation is that Tyr-89, in addition to hydrogen bonding to the quinone, is a proton donor during quinone reduction. We suggest that, as originally proposed for the *E. coli* SdhC Tyr-83 [2], Tyr-89 donates a proton to the O1 carbonyl of the quinone during the formation of ubiquinol and that protonation is essential for efficient catalysis. The residual activities of the Tyr-89 mutants in quinone reduction are likely due to the presence of inefficient alternate proton donors or water.

Mutations in the human *SDHD* gene are associated with the development of paragangliomas and pheochromocytomas. It has been suggested that these tumors develop because of an SDH-mediated increased generation of reactive oxygen species [17]. Specific mutations that affect the quinone-binding sites in the *C. elegans* complex II [12,15], in the *E. coli* fumarate reductase [33] or in the yeast SDH [22] do produce oxidative stress. We modeled the human SDHD Y114C mutation, which is associated with paraganglioma and carotid body tumors [34]. The yeast Sdh4p Y89C mutation does not greatly impair SDH assembly but it results in a complete loss of quinone reductase activity. Mitochondria from the Y89C mutant produce 7–8 fold less superoxide than wild type mitochondria (Table 5). The Y89C mutant is not hypersensitive to paraquat, also suggesting it is not under superoxide stress (results not shown). The mutant is however somewhat sensitive to hyperoxia on SGal medium, suggesting there may be some generation of reactive oxygen species other than superoxide under specific growth conditions. A likely source of these reactive oxygen species would be the flavin located at the active site [35]. Our results do not support a model that involves the SDH-mediated generation of superoxide free radicals as the cause of paraganglioma. Rather, the Y89C mutant with its complete loss of activity, likely leads to elevated levels of succinate and the induction of hypoxia-inducing factor [18,19]. This latter model also provides a plausible explanation for paraganglioma alleles that truncate or eliminate one of the SDH subunits and likely prevent enzyme assembly [9].

In summary, our results indicate that Tyr-89 performs an essential step in ubiquinone reduction. We propose that Tyr-89 is a proton donor to the O1 carbonyl of the quinone. Our data also argue against a role for elevated production of reactive oxygen species in tumor formation.

Acknowledgement

This work was supported by the Canadian Institutes of Health Research (MT-15290, to B.D.L.).

References

[1] B.D. Lemire, K.S. Oyedotun, The *Saccharomyces cerevisiae* mitochondrial succinate:ubiquinone oxidoreductase, Biochim. Biophys. Acta 1553 (2002) 102–116.
[2] V. Yankovskaya, R. Horsefield, S. Tornroth, C. Luna-Chavez, H. Miyoshi, C. Leger, B. Byrne, G. Cecchini, S. Iwata, Architecture of succinate dehydrogenase and reactive oxygen species generation, Science 299 (2003) 700–704.
[3] R. Horsefield, V. Yankovskaya, G. Sexton, W. Whittingham, K. Shiomi, S. Omura, B. Byrne, G. Cecchini, S. Iwata, Structural and computational analysis of the quinone-binding site of complex II (succinate–ubiquinone oxidoreductase): a mechanism of electron transfer and proton conduction during ubiquinone reduction, J. Biol. Chem. 281 (2006) 7309–7316.
[4] F. Sun, X. Huo, Y. Zhai, A. Wang, J. Xu, D. Su, M. Bartlam, Z. Rao, Crystal structure of mitochondrial respiratory membrane protein complex II, Cell 121 (2005) 1043–1057.
[5] L.S. Huang, G. Sun, D. Cobessi, A.C. Wang, J.T. Shen, E.Y. Tung, V.E. Anderson, E.A. Berry, 3-Nitropropionic acid Is a suicide inhibitor of mitochondrial respiration that, upon oxidation by complex II, forms a covalent adduct with a catalytic base arginine in the active site of the enzyme, J. Biol. Chem. 281 (2006) 5965–5972.
[6] K.S. Oyedotun, B.D. Lemire, The quaternary structure of the *Saccharomyces cerevisiae* succinate dehydrogenase: homology modeling, cofactor docking, and molecular dynamics simulation studies, J. Biol. Chem. 279 (2004) 9424–9431.
[7] B.E. Baysal, R.E. Ferrell, J.E. Willett-Brozick, E.C. Lawrence, D. Myssiorek, A. Bosch, A. van der Mey, P.E. Taschner, W.S. Rubinstein, E.N. Myers, C.W. Richard III, C.J. Cornelisse, P. Devilee, B. Devlin, Mutations in *SDHD*, a mitochondrial complex II gene, in hereditary paraganglioma, Science 287 (2000) 848–851.
[8] B.E. Baysal, J.E. Willett-Brozick, E.C. Lawrence, C.M. Drovdlic, S.A. Savul, D.R. McLeod, H.A. Yee, D.E. Brackmann, W.H. Slattery III, E.N. Myers, R.E. Ferrell, W.S. Rubinstein, Prevalence of SDHB, SDHC, and SDHD germline mutations in clinic patients with head and neck paragangliomas, J. Med. Genet. 39 (2002) 178–183.
[9] C. Eng, M. Kiuru, M.J. Fernandez, L.A. Aaltonen, A role for mitochondrial enzymes in inherited neoplasia and beyond, Nat. Rev., Cancer 3 (2003) 193–202.
[10] P. Rustin, A. Rötig, Inborn errors of complex II — unusual human mitochondrial diseases, Biochim. Biophys. Acta 1553 (2002) 117–122.
[11] B.E. Baysal, Hereditary paraganglioma targets diverse paraganglia, J. Med. Genet. 39 (2002) 617–622.
[12] N. Ishii, M. Fujii, P.S. Hartman, M. Tsuda, K. Yasuda, N. Senoo-Matsuda, S. Yanase, D. Ayusawa, K. Suzuki, A mutation in succinate dehydrogenase cytochrome b causes oxidative stress and ageing in nematodes, Nature 394 (1998) 694–697.
[13] S. Melov, J. Ravenscroft, S. Malik, M.S. Gill, D.W. Walker, P.E. Clayton, D.C. Wallace, B. Malfroy, S.R. Doctrow, G.J. Lithgow, Extension of lifespan with superoxide dismutase/catalase mimetics, Science 289 (2000) 1567–1569.
[14] N. Senoo-Matsuda, P.S. Hartman, A. Akatsuka, S. Yoshimura, N. Ishii, A complex II defect affects mitochondrial structure, leading to *ced-3*- and *ced-4*-dependent apoptosis and aging, J. Biol. Chem. 278 (2003) 22031–22036.
[15] N. Senoo-Matsuda, K. Yasuda, M. Tsuda, T. Ohkubo, S. Yoshimura, H. Nakazawa, P.S. Hartman, N. Ishii, A defect in the cytochrome *b* large subunit in complex II causes both superoxide anion overproduction and abnormal energy metabolism in *Caenorhabditis elegans*, J. Biol. Chem. 276 (2001) 41553–41558.
[16] E. Gottlieb, I.P. Tomlinson, Mitochondrial tumour suppressors: a genetic and biochemical update, Nat. Rev., Cancer 5 (2005) 857–866.
[17] P. Rustin, A. Munnich, A. Rötig, Succinate dehydrogenase and human diseases: new insights into a well-known enzyme, Eur. J. Hum. Genet. 10 (2002) 289–291.
[18] J.J. Brière, J. Favier, P. Bénit, V.E. Ghouzzi, A. Lorenzato, D. Rabier, M.F. Di Renzo, A.P. Gimenez-Roqueplo, P. Rustin, Mitochondrial succinate is

instrumental for HIF1α nuclear translocation in SDHA-mutant fibroblasts under normoxic conditions, Hum. Mol. Genet. 14 (2005) 3263–3269.
[19] M.A. Selak, S.M. Armour, E.D. MacKenzie, H. Boulahbel, D.G. Watson, K.D. Mansfield, Y. Pan, M.C. Simon, C.B. Thompson, E. Gottlieb, Succinate links TCA cycle dysfunction to oncogenesis by inhibiting HIF-alpha prolyl hydroxylase, Cancer Cell 7 (2005) 77–85.
[20] K.S. Oyedotun, B.D. Lemire, The quinone-binding sites of the *Saccharomyces cerevisiae* succinate-ubiquinone oxidoreductase, J. Biol. Chem. 276 (2001) 16936–16943.
[21] E. Dibrov, S. Fu, B.D. Lemire, The *Saccharomyces cerevisiae* TCM62 gene encodes a chaperone necessary for the assembly of the mitochondrial succinate dehydrogenase (complex II), J. Biol. Chem. 273 (1998) 32042–32048.
[22] J. Guo, B.D. Lemire, The ubiquinone-binding site of the *Saccharomyces cerevisiae* succinate-ubiquinone oxidoreductase is a source of superoxide, J. Biol. Chem. 278 (2003) 47629–47635.
[23] G. Sarkar, S.S. Sommer, The "megaprimer" method of site-directed mutagenesis, BioTechniques 8 (1990) 404–407.
[24] D. Van Der Spoel, E. Lindahl, B. Hess, G. Groenhof, A.E. Mark, H.J. Berendsen, GROMACS: fast, flexible, and free, J. Comput. Chem. 26 (2005) 1701–1718.
[25] D.P. Tieleman, H.J. Berendsen, Molecular dynamics simulations of fully hydrated DPPC with different macroscopic boundary conditions and parameters, J. Chem. Phys. 105 (1996) 4871–4880.
[26] J. Funahashi, Y. Sugita, A. Kitao, K. Yutani, How can free energy component analysis explain the difference in protein stability caused by amino acid substitutions? Effect of three hydrophobic mutations at the 56th residue on the stability of human lysozyme, Protein Eng. 16 (2003) 665–671.
[27] K.S. Oyedotun, B.D. Lemire, The carboxyl terminus of the *Saccharomyces cerevisiae* succinate dehydrogenase membrane subunit, SDH4p, is necessary for ubiquinone reduction and enzyme stability, J. Biol. Chem. 272 (1997) 31382–31388.
[28] B.L. Bullis, B.D. Lemire, Isolation and characterization of the *Saccharomyces cerevisiae* SDH4 gene encoding a membrane anchor subunit of succinate dehydrogenase, J. Biol. Chem. 269 (1994) 6543–6549.
[29] J.P. Bayley, P. Devilee, P.E. Taschner, The SDH mutation database: an online resource for succinate dehydrogenase sequence variants involved in pheochromocytoma, paraganglioma and mitochondrial complex II deficiency, BMC Med. Genet. 6 (2005) 39.
[30] K.M. Robinson, A. von Kieckebusch-Gück, B.D. Lemire, Isolation and characterization of a *Saccharomyces cerevisiae* mutant disrupted for the succinate dehydrogenase flavoprotein subunit, J. Biol. Chem. 266 (1991) 21347–21350.
[31] C.N. Pace, B.A. Shirley, M. McNutt, K. Gajiwala, Forces contributing to the conformational stability of proteins, FASEB J. 10 (1996) 75–83.
[32] K.S. Oyedotun, B.D. Lemire, The *Saccharomyces cerevisiae* succinate-ubiquinone oxidoreductase. Identification of Sdh3p amino acid residues involved in ubiquinone binding, J. Biol. Chem. 274 (1999) 23956–23962.
[33] G. Cecchini, H. Sices, I. Schröder, R.P. Gunsalus, Aerobic inactivation of fumarate reductase from *Escherichia coli* by mutation of the [3Fe–4S]-quinone binding domain, J. Bacteriol. 177 (1995) 4587–4592.
[34] J.M. Milunsky, T.A. Maher, V.V. Michels, A. Milunsky, Novel mutations and the emergence of a common mutation in the *SDHD* gene causing familial paraganglioma, Am. J. Med. Genet. 100 (2001) 311–314.
[35] K.R. Messner, J.A. Imlay, Mechanism of superoxide and hydrogen peroxide formation by fumarate reductase, succinate dehydrogenase, and aspartate oxidase, J. Biol. Chem. 277 (2002) 42563–42571.
[36] Y.C. Sun, D.L. Veenstra, P.A. Kollman, Free energy calculations of the mutation of Ile96→Ala in barnase: contributions to the difference in stability, Protein Eng. 9 (1996) 273–281.